

# Solution, Thermal and Optical Properties of Novel Poly(pyridinium salt)s Derived from Conjugated Pyridine Diamines\*

ALEXI K. NEDELTCHEV, HAESOOK HAN, PRADIP K. BHOWMIK

Department of Chemistry, University of Nevada Las Vegas, 4505 Maryland Parkway, Las Vegas NV 89154-4003, USA

Received 21 May 2010; accepted 4 July 2010

DOI: 10.1002/pola.24228

Published online in Wiley Online Library (wileyonlinelibrary.com).

**ABSTRACT:** Several novel poly(pyridinium salt)s with heterocyclic pyridine moieties in their backbones with tosylate and triflimide counterions were prepared by either ring-transmutation polymerization reaction of phenylated-bis(pyrylium tosylate) with isomeric pyridine diamines of 4-phenyl-2,6-bis(4-aminophenyl)pyridine in dimethyl sulfoxide (DMSO) for 48 h at 130–140 °C or by metathesis reaction of the respective tosylate polymers with lithium triflimide in DMSO at about 60 °C. Their chemical structures were characterized by FTIR, <sup>1</sup>H, <sup>13</sup>C NMR spectroscopy, and elemental analysis. Their number-average molecular weights (*M<sub>n</sub>*) were in the range of 8,000–51,000 and their polydispersities in the range of 1.18–2.13 as determined by gel permeation chromatography. They had excellent thermal stabilities of 340–458 °C and high glass transition temperatures >200 °C. As they showed good solubilities in common

organic solvents, their solution properties were also characterized for their lyotropic liquid-crystalline properties with polarizing optical microscopy (POM) studies. Their photoluminescent properties were examined by using a spectrofluorometer in both solution and solid states. Their quantum yields were rather low, which were in the range of 1.3–2.0%. Additionally, hand-drawn fibers from the melts were examined to determine their morphologies with a number of microscopic techniques including POM, scanning electron microscopy, and transmission electron microscopy. © 2010 Wiley Periodicals, Inc. *J Polym Sci Part A: Polym Chem* 48: 4408–4418, 2010

**KEYWORDS:** gel permeation chromatography; LCPs; luminescence; lyotropic; poly(pyridinium salt)s; TEM, UV-vis spectroscopy

**INTRODUCTION** Light-emitting,  $\pi$ -conjugated compounds, oligomers, and polymers have received a lot of attention for the preparation of semiconductors for applications in micro- and optoelectronic devices, such as organic light emitting diodes (OLEDs), organic field-effect transistors (OFETs), organic photovoltaic cells (OPVs), and organic lasers.<sup>1</sup> Among these, nitrogen-containing conjugated materials have shown considerable promise as an electron transporting layers (ETLs) in OLEDs. They have high electron affinities because they have electron-deficient heterocycles and can effectively transport electrons from the cathode throughout the ETL materials until they successfully recombine with holes resulting in light emission.<sup>2–4</sup> Moreover, it is demonstrated that their light-emitting properties could be tuned through the protonation of nitrogen heterocycles.<sup>2b,c,3f</sup> Different heterocyclic moieties, such as oxadiazole,<sup>3a</sup>azole,<sup>3b</sup>benzobisazole,<sup>3c</sup>benzothiadiazole,<sup>3d</sup>pyridine,<sup>3e</sup>quinoxaline,<sup>3f</sup>quinoline,<sup>3g</sup>and anthrazoline<sup>3h</sup> were incorporated in both molecular and polymeric materials that were comprehensively reviewed by Jenekhe et al.<sup>4</sup> The 4-phenyl-2,6-bis(4-aminophenyl)pyridine, prepared by Chichibabin reaction, and its derivatives were used in the synthesis of various classes of polymers including polyamides, polyimides, poly(amide-imide)s, and poly-

(ester-imide)s.<sup>5–7</sup> They showed good thermal stabilities and high thermal transitions; however, they were soluble only in high boiling solvents, such as dimethyl sulfoxide (DMSO), *N*-methyl-2-pyrrolidone (NMP), *N,N*-dimethylacetamide (DMAc), and *m*-cresol, which makes their processability cumbersome. There are only a few examples that exhibit light emitting properties after protonation but not in their neutral forms.<sup>8</sup>

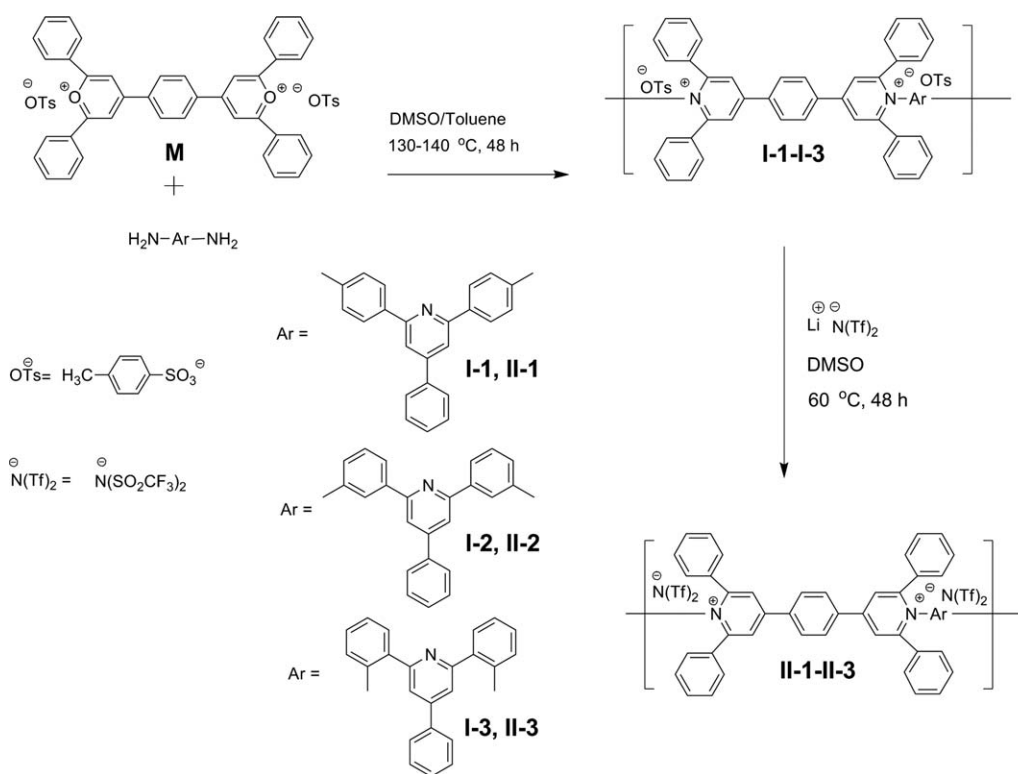
Two key methods that are generally applied to improve polymers solubilities include attachment of flexible alkyl chains as pendant groups as well as incorporation of kinks and twists in the  $\pi$ -conjugated moieties. Another method of achieving high solubility of a polymer is to introduce ionic charges in the backbone of the polymer chain. Such are the examples of viologen polymers and poly(pyridinium salt)s.<sup>9–11</sup> The high solubility is usually achieved by solvation of ionic charges in the polymer chain as well as of counterions resulting in substantial increase in their solubility in polar solvents. Additionally, variation of different sizes of counterions could result in a substantial change of their solubility in various organic solvents.<sup>11</sup>

Because the conception of poly(pyridinium salt)s, they have undergone significant improvements with regard to synthesis

\*This article is dedicated to the late Professor Robert W. Lenz (1926–2010).

Additional Supporting Information may be found in the online version of this article. Correspondence to: P. K. Bhowmik (E-mail: pradip.bhowmik@unlv.edu)

*Journal of Polymer Science: Part A: Polymer Chemistry*, Vol. 48, 4408–4418 (2010) © 2010 Wiley Periodicals, Inc.



**SCHEME 1** Synthesis of poly(pyridinium salt)s.

and physical properties. Initially, they had very low molecular weights, limited solubility, and low thermal stability.<sup>9</sup> Harris et al. were able to modify the procedure of the ring-transmutation polymerization reaction by using DMSO as a reaction medium thereby significantly improving their molecular weights.<sup>10a</sup> Their solubility and thermal stability were significantly improved with the introduction of organic counterions for the main-chain ionic polymers.<sup>10b,11a,b</sup> In recent years, we have continuously explored various poly(pyridinium salt)s containing both aromatic and aliphatic moieties for their various interesting properties.<sup>11</sup> They exhibited photoluminescence in various organic solvents as well as film states ranging from UV to green light.<sup>11d</sup> Moreover, they are amorphous having glass transition temperatures  $T_g > 150$  °C even for polymers with oxyalkylene units in their main chains.<sup>11f,g</sup> These ionenes are thermally robust with decomposition temperatures ( $T_d$ )  $> 400$  °C<sup>11a-d</sup> for fully aromatic polymers and  $T_d > 200$  °C<sup>11e</sup> for alkyl ones. They could be easily processed into thin films and multilayer assemblies because they are polycations having excellent solubility in common organic solvents. Furthermore, they exhibit liquid-crystalline (LC) properties both thermotropic (in melt) and lyotropic (in solution).<sup>11</sup> This combination of properties makes these polymers potential candidates for various opto-electronic applications, such as charge-transporting materials in OLEDs or materials for LECs. In this article, we describe the synthesis of a new series of wholly aromatic poly(pyridinium salt)s, with tosylate and triflimide counterions, having pyridine isomeric diamine units in their backbones and characterize their physical properties by using a number of experimental techniques. The

general structures and designations of these ionic polymers used in this study are outlined in Scheme 1.

## EXPERIMENTAL

### Materials

3'-nitroacetophenone, 4'-nitroacetophenone, ammonium acetate, and 10% Pd/C were purchased from Sigma-Aldrich. The 2'-nitroacetophenone and hydrazine monohydrate were purchased from TCI, America. Lithium triflimide and common solvents and deuterated solvents were procured from Fisher Scientific. All of the chemicals from various vendors were used as received.

### Monomer Synthesis

The 4,4'-(1,4-phenylene)bis(2,6-diphenylpyridinium)ditosylate, **M**, was synthesized according to the known procedure.<sup>11a</sup> A synthetic scheme for the preparation of isomeric pyridine diamines is provided in the Supporting Information for convenience and their general synthetic procedures are described below.

### Synthesis of 4-Phenyl-2,6-bis(4-nitrophenyl)pyridine

A total of 10.0 g (60.5 mmol) 4'-nitroacetophenone, 3.21 g (30.6 mmol) benzaldehyde, and 30.0 g ammonium acetate were heated to reflux in 75.0 mL of acetic acid for 2 h. As the reaction progressed, the solution changed from light yellow to dark red and eventually a precipitate formed. Upon cooling, the reaction mixture was poured into 50% acetic acid solution. It was collected and washed with hot ethanol. The compound was recrystallized from *N,N*-dimethylformamide (DMF). An amount of

3.30 g (8.30 mmol, 28% yield) of final product was collected having the  $T_m = 314$  °C at peak maximum.  $^1\text{H}$  NMR (400 MHz,  $d_6$ -DMSO)  $\delta$  ppm 8.54 (d,  $J = 8.8$  Hz, 4H), 8.40–8.24 (m, 6H), 8.05–7.98 (m, 2H), 7.62–7.48 (m, 3H).  $^{13}\text{C}$  NMR (100 MHz,  $d_6$ -DMSO)  $\delta$  ppm 155.5, 151.2, 149.0, 145.2, 137.8, 129.5, 129.1, 128.8, 124.5, 124.3, 119.8, 119.5. Anal. Calcd. for  $\text{C}_{23}\text{H}_{15}\text{N}_3\text{O}_4$  (397.40): C, 69.52; H, 3.80; N, 10.57. Found: C, 69.28; H, 4.14; N, 10.57.

#### 4-Phenyl-2,6-bis(3-nitrophenyl)pyridine

Yield = 25%, recrystallized from DMF having the  $T_m = 242$  °C at peak maximum.  $^1\text{H}$  NMR (400 MHz,  $d_6$ -DMSO)  $\delta$  ppm 9.01 (t,  $J = 1.90$  Hz, 2H), 8.70 (t,  $J = 14.11$  Hz, 2H), 8.30 (s, 2H), 8.26 (m, 2H), 8.02 (dd,  $J = 5.18, 3.10$  Hz, 2H), 7.80 (t,  $J = 7.98$  Hz, 2H), 7.61–7.45 (m, 3H).  $^{13}\text{C}$  NMR (100 MHz,  $d_6$ -DMSO)  $\delta$  ppm 155.3, 151.2, 149.5, 141.0, 137.8, 134.0, 133.7, 131.0, 130.4, 129.4, 128.1, 124.5, 122.2, 121.9, 118.9. Anal. Calcd. for  $\text{C}_{23}\text{H}_{15}\text{N}_3\text{O}_4$  (397.40): C, 69.52; H, 3.80; N, 10.57. Found: C, 69.31; H, 3.99; N, 10.61.

#### 4-Phenyl-2,6-bis(2-nitrophenyl)pyridine

Yield = 12%, recrystallized from acetonitrile having the  $T_m = 203$  °C at peak maximum.  $^1\text{H}$  NMR (400 MHz,  $\text{CDCl}_3$ )  $\delta$  ppm 7.93 (d,  $J = 7.86$  Hz, 2H), 7.78–7.64 (m, 8H), 7.54 (m, 5H).  $^{13}\text{C}$  NMR (100 MHz,  $\text{CDCl}_3$ )  $\delta$  ppm 156.0, 150.7, 149.4, 137.8, 135.2, 132.9, 131.9, 129.8, 129.7, 129.5, 127.5, 124.6, 120.4. Anal. Calcd. for  $\text{C}_{23}\text{H}_{15}\text{N}_3\text{O}_4$  (397.40): C, 69.52; H, 3.80; N, 10.57. Found: C, 69.52; H, 4.08; N, 10.78.

#### Synthesis of 4-Phenyl-2,6-bis(4-aminophenyl)pyridine

Ethanol suspension (50.0 mL) of the 3.10 g (78.0 mmol) 4-phenyl-2,6-bis(4-nitrophenyl) pyridine was heated to 50 °C in presence of 0.10 g of Pd/C and 5.00 mL of hydrazine monohydrate was added over 30 min as the reaction proceeded the solution cleared up. The reaction was kept at reflux for another 12 h. After completion, the reaction mixture was filtered over Celite twice to remove the Pd/C catalyst. The compound was recrystallized from ethanol to yield 2.05 g (20.9 mmol, yield 78%) having the  $T_m = 199$  °C at peak maximum.  $^1\text{H}$  NMR (400 MHz,  $d_6$ -DMSO)  $\delta$  ppm 8.01 (d,  $J = 8.62$  Hz, 4H), 7.95 (dd,  $J = 5.23, 3.27$  Hz, 2H), 7.80 (s, 2H), 7.59–7.45 (m, 3H), 6.68 (t,  $J = 8.8$  Hz, 4H), 5.43 (d,  $J = 7.55$  Hz, 4H).  $^{13}\text{C}$  NMR (100 MHz,  $d_6$ -DMSO)  $\delta$  ppm 157.2, 150.6, 149.3, 139.2, 129.7, 129.5, 128.5, 128.4, 127.7, 127.2, 114.3, 113.4. Anal. Calcd. for  $\text{C}_{23}\text{H}_{19}\text{N}_3$  (337.43): C, 81.87; H, 5.68; N, 12.45. Found: C, 81.59; H, 5.75; N, 12.69.

#### 4-Phenyl-2,6-bis(3-aminophenyl)pyridine

Yield = 92%, recrystallized from ethanol having the  $T_m = 178$  °C at peak maximum.  $^1\text{H}$  NMR (400 MHz,  $d_6$ -DMSO)  $\delta$  ppm 7.98 (m, 4H), 7.62–7.54 (m, 2H), 7.54–7.49 (m, 3H), 7.43 (m, 2H), 7.23–7.16 (t,  $J = 8.0$  Hz, 2H), 6.69 (ddd,  $J = 7.92, 2.28, 0.87$  Hz, 2H), 5.36–5.12 (s, 4H).  $^{13}\text{C}$  NMR (100 MHz,  $d_6$ -DMSO)  $\delta$  ppm 157.9, 149.7, 149.6, 140.3, 138.7, 129.8, 127.8, 116.8, 115.5, 115.4, 113.1. Anal. Calcd. for  $\text{C}_{23}\text{H}_{19}\text{N}_3$  (337.43): C, 81.87; H, 5.68; N, 12.45. Found: C, 81.49; H, 5.79; N, 12.48.

#### 4-Phenyl-2,6-bis(2-aminophenyl)pyridine

Yield = 89%, recrystallized from ethanol having the  $T_m = 172$  °C at peak maximum.  $^1\text{H}$  NMR (400 MHz,  $d_6$ -DMSO)

$\delta$  ppm 8.01–7.91 (m, 2H), 7.88 (s, 2H), 7.69 (dd,  $J = 7.82, 1.44$  Hz, 2H), 7.61–7.47 (m, 3H), 7.21–7.11 (m, 2H), 6.83 (dd,  $J = 8.12, 1.02$  Hz, 2H), 6.75–6.66 (dt,  $J = 7.4, 1.2$  Hz, 2H), 6.21 (s, 4H).  $^{13}\text{C}$  NMR (100 MHz,  $d_6$ -DMSO)  $\delta$  ppm 158.6, 150.1, 147.8, 138.8, 130.5, 130.4, 129.9, 129.8, 128.0, 122.2, 118.2, 117.1, 116.9. Anal. Calcd. for  $\text{C}_{23}\text{H}_{19}\text{N}_3$  (337.43): C, 81.87; H, 5.68; N, 12.45. Found: C, 82.06; H, 5.66; N, 12.48.

#### Polymer Synthesis

##### Synthesis of Polymers I-1-I-3

The bis(pyrylium) salt was reacted with an appropriate diamine by a ring-transmutation reaction to yield each of the desired polymers. Equal mole ratio of each of monomers was placed in three-necked, round-bottomed flask equipped with a magnetic stirrer in DMSO. About 5 mL of toluene was added to remove the water generated in the reaction by forming a toluene/water azeotrope, which was facilitated by using Dean-Stark trap and water condenser. The temperature was monitored with a mercury thermometer and adjusted to 130–135 °C for polymerization reaction. The reaction was kept under nitrogen atmosphere for 48 h. Upon completion of the polymerization reaction, the contents of the reaction mixture were allowed to cool down to room temperature. The DMSO was subsequently removed from the reaction mixture *in vacuo* to form a viscous polymer solution. It was then poured into water to precipitate the polymer, which was then filtered to collect it. It was additionally washed a few times with boiling water to remove DMSO completely. The resulting polymer was dried *in vacuo* at 110 °C for 72 h. Data for polymer **I-1**: Anal. Calcd. for  $\text{C}_{77}\text{H}_{57}\text{N}_3\text{O}_6\text{S}_2$  (1184.45): C, 78.08; H, 4.85; N, 3.55; O, 8.11; S, 5.41. Found: C, 73.73; H, 5.53; N, 3.40; S, 5.39; for polymer **I-2**: Anal. Calcd. for  $\text{C}_{77}\text{H}_{57}\text{N}_3\text{O}_6\text{S}_2$  (1184.45): C, 78.08; H, 4.85; N, 3.55; O, 8.11; S, 5.41. Found: C, 74.24; H, 5.56; N, 3.45; S, 5.77; and for polymer **I-3**: Anal. Calcd. for  $\text{C}_{77}\text{H}_{57}\text{N}_3\text{O}_6\text{S}_2$  (1184.45): C, 78.08; H, 4.85; N, 3.55; O, 8.11; S, 5.41. Found: C, 77.27; H, 6.11; N, 3.65; S, 5.95.

##### Synthesis of Polymers II-1-II-3

Polymers **II-1-II-3** were prepared by a metathesis reaction from the respective tosylate polymers with excess lithium triflimide salt in DMSO at 50 °C for 48 h. At the end of the metathesis reaction, the DMSO solvent was reduced *in vacuo* to form a viscous solution, and it was then poured into water to precipitate out the polymer. This procedure was repeated once or twice until all the tosylate counterions were exchanged to triflimide counterions, which was monitored by the analysis of  $^1\text{H}$  NMR spectrum. After the final precipitation, each polymer was washed extensively with boiling water to remove any residual organic salts and entrapped DMSO after which it was dried *in vacuo* at 110 °C for 72 h. Data for polymer **II-1**: Anal. Calcd. for  $\text{C}_{67}\text{H}_{43}\text{N}_5\text{O}_8\text{S}_2\text{F}_{12}$  (1402.34): C, 57.39; H, 3.09; N, 4.99; O, 9.13; S, 9.14; F, 16.26. Found: C, 57.36; H, 3.33; N, 5.12; S, 9.29; Polymer **II-2**: Anal. Calcd. for  $\text{C}_{67}\text{H}_{43}\text{N}_5\text{O}_8\text{S}_2\text{F}_{12}$  (1402.34): C, 57.39; H, 3.09; N, 4.99; O, 9.13; S, 9.14; F, 16.26. Found: C, 57.39; H, 3.66; N, 5.00; S, 8.98; and Polymer **II-3**: Anal. Calcd. for  $\text{C}_{67}\text{H}_{43}\text{N}_5\text{O}_8\text{S}_2\text{F}_{12}$  (1402.34): C, 57.39; H,

3.09; N, 4.99; O, 9.13; S, 9.14; F, 16.26. Found: C, 59.30; H, 3.70; N, 5.00; S, 8.83.

### Polymer Characterization

The  $^1\text{H}$  and  $^{13}\text{C}$  NMR spectra were recorded with a Varian NMR 400 spectrometer equipped with three RF channels operating at 400 and 100 MHz, respectively. Polymer solutions were prepared by dissolving 35–40 mg of polymers per mL of  $d_6$ -DMSO with TMS as an internal standard. FTIR spectra were recorded with a Shimadzu spectrometer. Polymer samples were prepared by coating NaCl plates with polymers, which were subsequently dried *in vacuo* at 70 °C overnight. The phase transition temperatures of monomers and polymers were measured using a TA 2100 differential scanning calorimetry (DSC) in nitrogen at heating and cooling rates of 10 °C/min. The temperature axis of the DSC thermogram was calibrated before using the reference standards of high purity indium and tin. Polymers of 8–10 mg were used in these measurements. Thermal stability of each of these polymers was analyzed by thermogravimetric analysis (TGA) using TA 2100 instrument at a rate of 10 °C/min in nitrogen using sample not less than 10 mg. The LC properties of both lyotropic and thermotropic were assessed using a polarized optical microscope (POM) Nikon Labophot 2 equipped with crossed polarizers and hot stage. The UV-Vis absorption spectra of polymer solutions in organic solvents were recorded using Varian Cary 50 Bio UV-Visible spectrophotometer in quartz cuvettes. Their photoluminescent properties in both solution and film states were analyzed using a Perkin Elmer LS-55 luminescence spectrophotometer. Quantum yields were analyzed by adjusting the solution absorption using the UV-Vis to about 0.05 at 350 nm wavelength. The outputs were then measured using the luminescence spectrophotometer at the same wavelength and compared it with known 9,10-diphenylanthracene standard using eq 1:

$$\phi_{\text{unk}} = \phi_{\text{std}} \left( \frac{I_{\text{unk}}}{I_{\text{std}}} \right) \left( \frac{A_{\text{std}}}{A_{\text{unk}}} \right) \left( \frac{\eta_{\text{unk}}}{\eta_{\text{std}}} \right)^2 \quad (1)$$

where  $f$  is the fluorescence quantum yield,  $I$  is the absorption of the excitation wavelength,  $A$  is the area under the emission curve, and  $h$  is the refractive index of the solvents used. Subscript std denotes the standard and subscript unk denotes the unknown.<sup>12</sup> To assess molecular weight of polymer, gel permeation chromatography (GPC) was run at 50 °C with a flow rate of 1 mL/min. The GPC instrument had connected with Water 515 pump together with a Viscotek Model 301 Triple Detector Array. The array contained a laser refractometer, a differential viscometer, and a light scattering detector both right angle laser light scattering (RALS) as well as low angle laser scattering (LALS) in a single instrument with a fixed interdetector and temperature control that can be regulated up to 80 °C. In this system, the molecular weight is available from light scattering and concentration detectors, whereas the latter combines with a viscosity detector to provide intrinsic viscosity  $[\eta]$ . The instrument was calibrated with a pullulan standard of P-50 obtained from Polymer Standard Services, USA. Separations were accom-

plished using ViscoGel I-MBHMW-3078 columns purchased from Viscotek. An aliquot of 100–200  $\mu\text{L}$  of 2 mg/mL polymer solution in DMSO containing 0.1 M LiBr was injected. The  $dn/dc$  values were corrected by injecting different volumes of polymers to assess their trends. All data analyses were performed by using Viscotek TriSEC software. The X-ray diffraction studies were performed on finely powdered samples at room temperature with a PANalytical X'PERT Pro X-ray diffraction spectrometer using Cu  $K\alpha$  radiation ( $\lambda = 1.5418 \text{ \AA}$ ) as an X-ray source operating at 45 kV and 40 mA. The scanning electron microscopy (SEM) images of hand-drawn fibers of polymers prepared from their melts were taken with the JXA-8900 SuperProbe. The transmission electron microscopy (TEM) studies of polymers were performed by using a TECNAI-F30-Super-twin TEM instrument operating at 300 kV field emission mode. For this study, a drop of 5 wt % of polymer I-2 in methanol was deposited on a copper grid coated with carbon film that is suitable for electron microscopy and the solvent was evaporated at room temperature. In the case of polymer I-3, a drop of 2 wt % in methanol was used in the deposition process.

## RESULTS AND DISCUSSION

### Chemical Structures

The chemical structures of the polymers in this study are consistent with the spectra of FTIR,  $^1\text{H}$  and  $^{13}\text{C}$  NMR spectroscopy, and elemental analysis. The FTIR spectrum showed the following representative characteristic peaks for polymer I-1: 3057 (C–H aromatic stretching), 1619–1448 (C=C and C=N aromatic ring stretching), 1200 (C–N<sup>+</sup>), 1120 (S=O asymmetric stretching), 1033–1010 (S=O symmetric stretching,  $d$ ), and 848–680  $\text{cm}^{-1}$  (C–H out-of-plane bending). Representative characteristic peaks for polymer II-1: 3065 (C–H aromatic stretching), 1619–1450 (C=C and C=N aromatic ring stretching), 1348 (C–F stretching), 1194 (C–N<sup>+</sup>), 1133 (S=O asymmetric stretching), 1058 (S=O symmetric stretching), and 844–698  $\text{cm}^{-1}$  (C–H out-of-plane bending). Vinylous signals in both  $^1\text{H}$  and  $^{13}\text{C}$  NMR spectra of polymers I-1–I-3 were not observed suggesting that the ring-transmutation polymerization reaction underwent to completion. Disappearance of the characteristic proton and carbon peaks of the tosylate counterion in the spectra of polymers II-1–II-2 suggested that the metathesis reaction also proceeds to completion. The  $^1\text{H}$  NMR spectra of polymers I-1 and II-1, which had para-linked pyridine diamine moieties in the polymer chains, had very broad proton signals similar to other high viscosity polymers. Furthermore, some of the carbon signals in their  $^{13}\text{C}$  NMR spectra did not resolve well due to their high viscosity character. The other polymers, which had meta- and ortho-linked pyridine diamine moieties, showed significantly the well-resolved features in their NMR spectra. All of the spectra for these polymers are provided in Supporting Information for detail analyses.

### Molecular Weight Determination

The molecular weight data for the polymers in this study are summarized in Table 1. Mark–Houwink constants  $\alpha$  and  $K$  as

**TABLE 1** GPC Data of Poly(pyridinium salt)s

Polymer	IV (dL/g)	$M_n$	$M_w$	$M_w/M_n$	$dn/dc$ (mL/g)	$\alpha^a$	$K^a$
<b>I-1</b>	0.38	50,952	60,339	1.18	0.1400	1.27	$3.21 \times 10^{-7}$
<b>II-1</b>	0.26	58,301	76,719	1.32	0.1000	0.99	$3.78 \times 10^{-6}$
<b>I-2</b>	1.23	48,133	94,692	1.97	0.2400	0.82	$1.19 \times 10^{-4}$
<b>II-2</b>	0.99	51,485	109,751	2.13	0.2000	0.80	$1.15 \times 10^{-4}$
<b>I-3</b>	0.05	7,674	11,042	1.44	0.1800	1.22	$6.19 \times 10^{-7}$
<b>II-3</b>	0.12	14,577	18,772	1.29	0.2200	1.16	$1.41 \times 10^{-6}$

<sup>a</sup>  $\alpha$  and  $K$  were calculated by using Mark-Houwink equation:  $[\eta] = KM^c$ .

well as  $dn/dc$  values are also included. Their intrinsic viscosities were distinctively related to their structures. Polymer **I-3**, which contained tosylate counterion and an ortho-linked pyridine diamine moiety in the main chain, had the lowest viscosity value of 0.05 dL/g. Notably, polymer **I-2**-meta-linked tosylate polymer had the highest viscosity value of 1.23 dL/g, which was significantly higher than the value for the polymer with para-linked pyridine diamine moieties. Neutral polyamides<sup>7a,c</sup> and polyesters<sup>5,7b</sup> based on 4-aryl-2,6-bis(4-aminophenyl)pyridine and 4-aryl-2,6-bis(4-chloro-carbonylphenyl)pyridine moieties, respectively, showed inherent viscosities of 0.32–0.49<sup>7a,c</sup> and 0.68–0.87,<sup>5,7b</sup> respectively. Number-average molecular weight ( $M_n$ ) was the lowest of 8,000 for polymer **I-3** and that was the highest of 58,000 for polymer **II-1**. Their weight-average molecular weights ( $M_w$ ) ranged from 11,000 to 110,000. The polydispersity indices ( $M_w/M_n$ ) of these polymers ranged from 1.18 to 2.13 (Table 1). Representative GPC plots of polymers **I-1** and **II-1** are provided in Supporting Information in Figure S19. Overall, they had a wide range of molecular weights, intrinsic viscosities and polydispersities. Nonetheless, their molecular weights are sufficiently high enough to assess their solutions, thermal and optical properties without concerns with regard to the effect of molecular weights on these properties.

### Solution Properties

Solubility of highly conjugated polymers is always limited due to their rigid structures. Therefore, their processability into thin films and fibers is indeed a challenging task. Notable example is Kevlar, which is a para-linked aramide, that is only soluble in concentrated sulfuric acid.<sup>13</sup> Even though, the poly(pyridinium salt)s in this study are highly conjugated they still had good solubility in common organic solvents, such as tetrahydrofuran (THF), methanol, acetonitrile, DMSO, among others, compared with neutral polyamides and poly-

esters based on 4-aryl-2,6-bis(4-phenyl)-pyridines, which are generally soluble only in high boiling solvents.<sup>5–7</sup> We were motivated to study their lyotropic LC properties, because there are many examples of poly(pyridinium salt)s exhibiting lyotropic LC phases, such as mosaic texture or Maltese crosses in various polar organic solvents.<sup>11</sup> As all of the polymers described here are based on different isomeric pyridine monomers, it is of significant interest to establish how structural differences would impact their solution properties (Table 2). This is particularly interesting, because the well-known polymer Kevlar forms lyotropic phase in strongly acid media including concentrated sulfuric acid, whereas Nomex, which is meta-linked aramide, does not self-assemble into a lyotropic phase.<sup>13</sup> Polymer **I-1**, which had a tosylate counterion and para-linked pyridine moiety, did not show solubility in methanol or acetonitrile but had a very good solubility in DMSO. Increase of the polymer concentration in DMSO eventually passed the critical concentration ( $C^*$ ) at 31 wt % and fully-grown lyotropic LC texture was observed as shown in Figure 1(a). On the other hand, polymer **II-1** containing triflimide as counterion showed improved solubility in acetonitrile and DMSO but not in methanol. A full grown lyotropic LC phase was developed in these solvents at 20 and 50 wt %, respectively. Figure 1(b) shows the lyotropic LC texture of polymer **II-2** in DMSO. Polymer **I-2**, which was the polymer with meta-linked pyridine diamine moiety and tosylate counterion, showed better solubility but some of the lyotropic LC had diminished. It was soluble in methanol and showed lyotropic LC phase above 30 wt % in this solvent. Biphasic solutions were observed in acetonitrile and DMSO. Polymer **II-2** containing triflimide counterion had very high solubilities in acetonitrile and DMSO but only isotropic solutions were observed, whereas in methanol a biphasic solution formed at low concentration of 5 wt %. The polymers **I-3** and **II-3**, which had an ortho-linked pyridine diamine moiety, had very high solubilities in methanol, acetonitrile, and

**TABLE 2** Solution Properties of Poly(pyridinium salt)s

Polymer	<b>I-1</b>	<b>II-1</b>	<b>I-2</b>	<b>II-2</b>	<b>I-3</b>	<b>II-3</b>
CH <sub>3</sub> OH ( $\epsilon = 32.6$ )	–	–	30% Lyotropic	5% Biphasic <sup>a</sup>	50% Biphasic <sup>a</sup>	10% Biphasic <sup>a</sup>
CH <sub>3</sub> CN ( $\epsilon = 37.5$ )	–	20% Lyotropic	10% Biphasic <sup>a</sup>	Up to 20% Isotropic	59% Biphasic <sup>a</sup>	Up to 50% Isotropic
DMSO ( $\epsilon = 48.9$ )	31% Lyotropic	50% Lyotropic	41% Biphasic <sup>a</sup>	Up to 30% Isotropic	Up to 50% Isotropic	Up to 50% Isotropic

<sup>a</sup> The coexistence of anisotropic (bright) and isotropic (dark) phase.

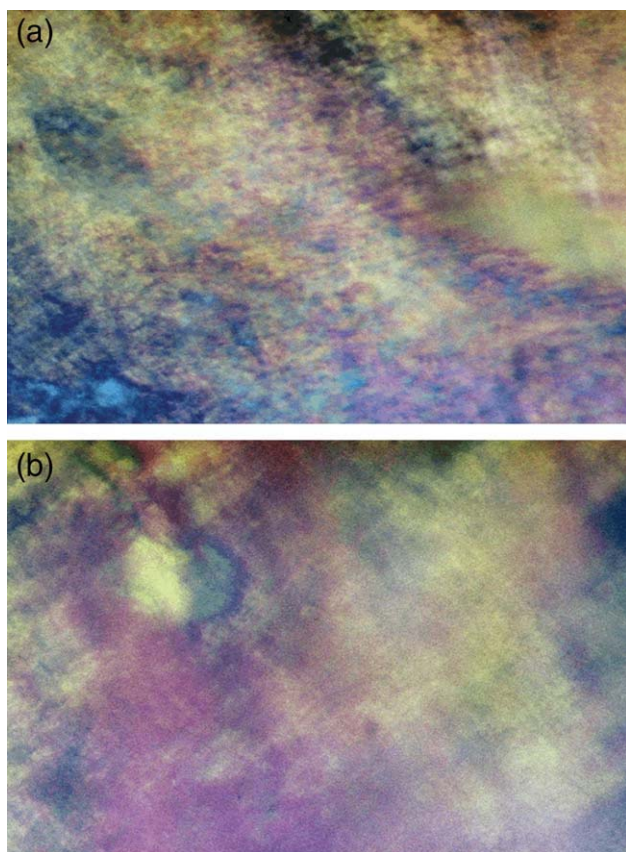


**FIGURE 1** Photomicrographs of (a) polymer **I-1** at 31 wt % in DMSO and (b) polymer **II-1** at 50 wt % in DMSO under crossed polarizers exhibiting lyotropic LC phases, respectively (magnification 400 $\times$ ). [Color figure can be viewed in the online issue, which is available at [wileyonlinelibrary.com](http://wileyonlinelibrary.com).]

DMSO but only biphasic solutions were observed at very high concentrations in several cases. Overall, two important trends stem from these results. First, the solubility was increased by introducing meta- and ortho-linked pyridine diamines but their lyotropic liquid crystal character decreased as is the case with Kevlar and Nomex. Second, the change in counterion from tosylate to triflimide of polymer increased the solubility in acetonitrile and DMSO but decreased in methanol.

## Thermal Properties

### Thermal Stability

High thermal stability is generally desirable for polymers that are used at high operating temperatures to extend their life time. To enhance it, highly  $\pi$ -conjugated aromatic and heterocyclic structures are introduced into polymer chains, but often they lead to poor solubility.<sup>4–8</sup> In this study, poly(pyridinium salt)s with heterocyclic pyridine diamine moieties were found to have excellent thermal stabilities in the range of 340–458  $^{\circ}\text{C}$ , while maintaining their solubility in common organic solvents (*vide supra*). Polymers with triflimide counterions had 87–102  $^{\circ}\text{C}$  higher thermal stability than the polymers with tosylate counterions (Fig. S20), which were in excellent agreements with the previous

results of other poly(pyridinium salt)s.<sup>11</sup> This characteristic may be attributed to the following two reasons. First, sodium tosylate (155  $^{\circ}\text{C}$ ) had much lower decomposition temperature than lithium triflimide (363  $^{\circ}\text{C}$ ). This trend is manifested in the degradation temperatures of these ionic polymers. These results are also supported by the study of the decomposition products of poly(pyridinium salt)s with tetrafluoroborate counterion, where the counterion decomposes before that of the main-chain polymer.<sup>10b</sup> Second, triflimide counterion has a significantly weaker nucleophilic character compared with tosylate and, therefore, it starts to act as a nucleophile to cause the decomposition of main-chain of the polymer at high temperature. A weight loss of 2–3% was observed in all tosylate polymers, which is due to a solvent loss (Fig. S20). The measured thermal properties of these polymers including decomposition and glass transition temperatures are summarized in Table 3.

### Thermal Transitions

Amorphous materials are a particularly interesting class of materials, because they are easy to process into thin films and fibers, they are transparent, they have no grain boundaries, they have homogenous properties and they have high quantum efficiencies.<sup>14</sup> For opto-electrical devices and other applications that operate at high temperature, high glass transition temperatures ( $T_g$ s) are required.<sup>4</sup> In their reviewed articles, Shirota et al. had identified a number of structural characteristics necessary to achieve a stable glassy state, while keeping high thermal stabilities.<sup>14</sup> These structural designs have been applied successfully in both molecular<sup>14</sup> and polymeric<sup>15</sup> materials. The synthesized ionic polymers had high  $T_g$ s as compiled in Table 3, similar to neutral polymers based on 4-aryl-2,6-bis(4-aminophenyl)-pyridine.<sup>5–7</sup> Polymer **I-1** had only one endotherm, which is attributed to solvent loss as supported by the TGA analysis (*vide supra*) and no other thermal transitions before its decomposition temperature, implying that this polymer had exceptionally high theoretical  $T_g$ . Polymer **II-1**, which was the triflimide adduct of polymer **I-1**, had a distinct  $T_g$  observed in all heating and cooling cycles at 324  $^{\circ}\text{C}$ . The polymers **I-2** and **II-2**, with meta-linked pyridine moiety, as expected, had distinctly lower  $T_g$ s at 285 and 251  $^{\circ}\text{C}$ , respectively. Finally, polymers **I-3** and **II-3** (Fig. S21) had the lowest  $T_g$ s 223 and 199  $^{\circ}\text{C}$ , respectively. Overall, two notable trends were clearly observed. Change of the counterion from tosylate to triflimide significantly lowered the glass transition temperature by 34  $^{\circ}\text{C}$  (polymer **I-2** vs. **II-2**) and 24  $^{\circ}\text{C}$  (polymer **I-3** vs. **II-3**). This decrease in  $T_g$  was presumably related to the fact that triflimide is a bulkier counterion compared with tosylate.

**TABLE 3** Thermal Properties of Poly(pyridinium salt)s

Polymer	<b>I-1</b>	<b>II-1</b>	<b>I-2</b>	<b>II-2</b>	<b>I-3</b>	<b>II-3</b>
$T_g^a$ ( $^{\circ}\text{C}$ )	–	324	285	251	223	199
$T_d^b$ ( $^{\circ}\text{C}$ )	365	458	355	457	340	427

<sup>a</sup> Glass transition was recorded from the second heating cycle of DSC thermogram.

<sup>b</sup> Thermal decomposition was recorded at 5 wt % loss in nitrogen.

**TABLE 4** Optical Properties of Poly(pyridinium salt)s

Polymer	I-1	II-1	I-2	II-2	I-3	II-3
UV abs (nm)	–	260,340	335	335	255,345	350
Band gap (eV)	–	3.23	3.27	3.27	3.20	3.22
PL $\lambda_{em}$ THF (nm)	–	–	–	–	–	483
PL $\lambda_{em}$ acetone (nm)	–	533	–	525	–	471
PL $\lambda_{em}$ CH <sub>3</sub> OH (nm)	–	–	489	–	477	–
PL $\lambda_{em}$ CH <sub>3</sub> CN (nm)	–	528	520	525	484	481
PL $\lambda_{em}$ film (nm)	–	490	521	474	460	455
$\phi_F$ (%) <sup>a</sup>	–	1.3	1.3	1.8	2.0	1.9

<sup>a</sup> Quantum yield was calculated against diphenyl anthracene as standard ( $\phi_F = 0.9$ ).

Similar trend was also observed in many ionic liquids where triflimide counterion lowered their melting points significantly.<sup>16</sup> Second trend was the decrease in  $T_g$  of these ionic polymers from para- to meta- to ortho-linked pyridine diamine moieties. This phenomenon is quite common in many classes of polymers, where kinks and twists are introduced in the main chain of polymers,<sup>13</sup> most notable examples of such properties are exhibited in the cases of para-linked Kevlar ( $T_g = 330$  °C) and meta-linked Nomex ( $T_g = 285$  °C) polymers.<sup>13c</sup>

### Optical Properties

Light emission in organic materials both molecular and polymeric ones have been of a significant interest in recent years for the development of various opto-electronic devices.<sup>1</sup> Introducing heterocyclic pyridine moieties not only improves thermal stabilities of materials but also provides tunability through protonation of the nitrogen heterocycle.<sup>2b,c,3f</sup> Many neutral polymers with 4-aryl-2,6-bis(phenyl)pyridine moieties were developed, which show interesting thermal properties,<sup>5–8</sup> but only a few of them were photoactive in their protonated and in their neutral states.<sup>8</sup> All of the polymers described herein, we introduced isomeric forms of 4-phenyl-2,6-bis(phenyl)pyridine in their backbones, because poly(pyridinium salt)s were already known for their interesting photoluminescent properties<sup>11</sup> and introduction of additional pyridine heterocyclic unit would help understand their light-emitting properties in both solution and solid states. Because of their good solubility the light-emitting properties of these polymers were studied in various solvents having a wide range of polarities ( $\epsilon = 7.5–37.5$ ). Their measured optical properties including UV-Vis, photoluminescence spectra and quantum yields are summarized in Table 4. Figure 2(a) displays photoluminescence spectra of tosylate polymers I-2 and I-3 in methanol. Note here that polymer I-1 had limited solubility in methanol that precluded the measurement of photoluminescence properties in this solvent. There was a slight bathochromic shift in the light emission of polymer I-2 compared with polymer I-3 exhibiting  $\lambda_{em}$  at 489 and 477 nm when excited with 375 and 380 nm light, respectively. This shift in light emission was probably because polymer I-2 had meta-linked pyridine moiety, whereas polymer I-3 had ortho-linked pyridine moiety. The  $\pi$ - $\pi$  stacking in polymer I-3 was precluded in contrast with polymer I-2, which resulted in less decrease in energy of the anti-

bonding  $\pi^*$  orbital that accounts for the hypsochromic shift. Figure 2(b) shows the light emission of the triflimide-containing polymers II-1–II-3. Polymers II-1 and II-2 emitted light in a similar range of  $\lambda_{em}$  at 528 and 525 nm when excited with 330 and 340 nm wavelength of light, respectively. Polymer II-3, similar to polymer I-3, was hypsochromically shifted exhibiting  $\lambda_{em}$  at 484 nm when excited with 335 nm light, compared with polymers II-1 and II-2. These results suggested that extensive kinks in the main chain had an effect on light emission. This phenomenon was consistent in different solvents and as well as with different counterions. In some cases, we observed a significant difference of light emission by simply changing the solvent. Such as the case with polymer I-2 that exhibited a bathochromic shift of 31 nm on changing from methanol to acetonitrile. These were the evidence for a solvatochromic effect. When considering the effect of counterions from tosylate to triflimide no appreciable change in light emission was detected in solution state. Polymers based on 4-aryl-2,6-bis(4-aminophenyl)pyridine are shown to have light emission in their protonated form using HCl exhibiting  $\lambda_{em}$  at 500 and 560 nm, which were in most cases bathochromically shifted compared with those of poly(pyridinium salt)s in this study.<sup>8</sup> Overall, the emission peaks of this series of poly(pyridinium salt)s had broad FWHM values over 100 nm. These optical properties were in excellent agreements with the FWHM values of other poly(pyridinium salt)s.<sup>11</sup> The large FWHM values are attributed to the fact that the light emission stemmed from more than one chromophoric species. Quantum yield is an important factor considering light emitting polymers (LEPs).<sup>1</sup> The polymers in this study had moderate quantum efficiencies ranging from 1.3 to 2.0%. The optical band gaps ( $E_g$ ) were determined from the onset values of UV-Vis absorption spectra. Their values ranged from 3.20–3.27 eV, which were comparable with previously reported poly(pyridinium salt)s<sup>11</sup> but generally lower than other  $\pi$ -conjugated LEPs.<sup>1b,c</sup> The poly(pyridinium salt)s in this study were made into thin films cast from acetonitrile, to study their light emitting properties in solid state. The photoluminescence spectra of the tosylate polymers I-2 and I-3 are displayed in Figure 2(c). They exhibited  $\lambda_{em}$  521 and 460 nm when excited at 390 and 340 nm light, respectively. There was a hypsochromic shift of 61 nm, which suggested that polymer I-3 had less ordered structures in solid state compared with polymer I-2, which also exhibited a hypsochromic shift

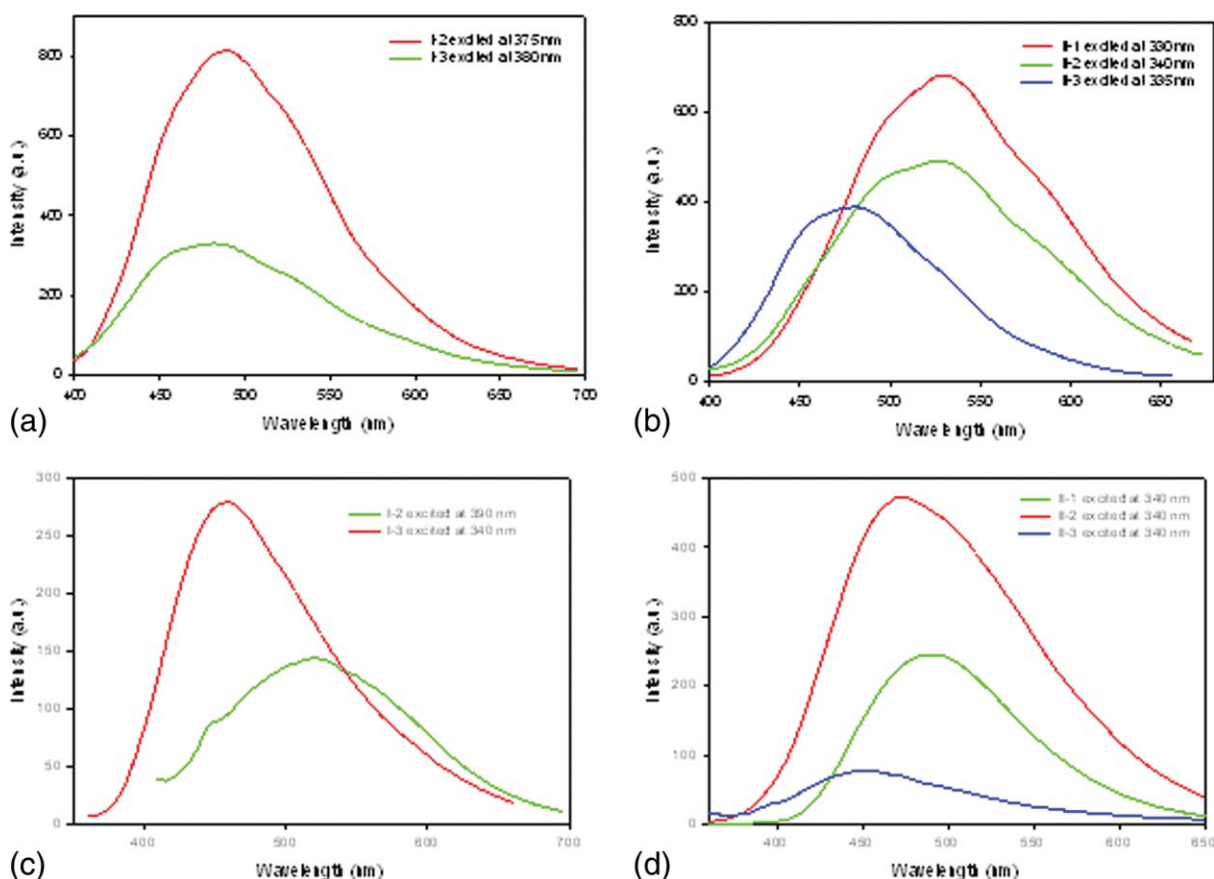


**FIGURE 2** Emission spectra of (a) polymers **I-2** and **I-3** in methanol, (b) polymers **II-1–II-3** in acetonitrile, (c) polymers **I-2** and **I-3** in thin films cast from methanol, and (d) polymers **II-1–II-3** in thin films cast from acetonitrile at various excitation wavelengths. [Color figure can be viewed in the online issue, which is available at [wileyonlinelibrary.com](http://wileyonlinelibrary.com).]

when compared with its solution spectrum. Figure 2(d) showed the spectra for the triflimide polymers where similar hypsochromic shifts were observed when going from para- to meta- to ortho-linked pyridine diamine moieties. They showed a  $\lambda_{em}$  at 490, 474, and 455 nm when excited at 340 nm wavelength of light. Exchanging the counterion had an effect on the light emission in film state. A difference of 47 nm between the light emission of polymers **I-2** and **II-2** was observed. The reason for this shift was presumably because triflimide prevented extensive  $\pi$ - $\pi$  stacking in the solid state. It is noteworthy that a significant change did not occur in the light emission of polymers **I-3** and **II-3** probably because these polymers had significantly disordered structures because they had ortho-linked pyridine diamine moieties in their main chains. In general, these polymers resulted in a significant hypsochromic shift when changing from solution to solid state. These results suggested that they were less ordered in film states compared with their solution spectra, which are in good agreement with the previously reported results of this class of poly(pyridinium salt)s.<sup>11</sup> The blue shifts in our ionic polymers, as opposed to red shifts of  $\pi$ -conjugated polymers in ordered structures, may be related to the fact that the extensive  $\pi$ - $\pi$  stacking phenomena of aromatic moieties do not occur in ionic polymers leading to less ordered structures presumably because of repulsive interactions of charges resulting in blue shifts.

### Morphology

As the polymers in this study are envisioned as materials for fabrication of different opto-electronic devices, we examined their microstructures with X-ray scattering and morphology with various microscopic techniques. Figure S22 shows the representative X-ray powder diffraction (XRD) plots of polymers **I-1–I-3** and **II-3** recorded at room temperature. They show broad diffraction peaks with relatively low intensities at both small and wide angles, which are the characteristic features of glassy phases of these ionic polymers. These results are in consistent with the DSC thermograms. These peaks can be assigned to the intermolecular short-range interactions that are parallel and perpendicular to the long axes of the polymer chains. The broad wide-angle diffraction peaks at around  $2\theta = 20^\circ$  that corresponded to the  $d$ -spacings in the range of 4.43–4.96 Å are the results of  $\pi$ - $\pi$  stacking of the polymer chains. The relative sharp, wide-angle diffraction peaks at around  $2\theta = 10^\circ$  that corresponded to the  $d$ -spacings in the range of 8.51–9.21 Å are related to some long-range order between the polymer chains. Thin films of these polymers were examined after annealing at temperatures above their glass transition temperatures. They had quite uniform textures. Figure 3(a–c) show photomicrographs of polymers **II-2**, **I-3**, and **II-3**, respectively. Polymers **I-3** and **II-3** exhibited some weak birefringent textures that

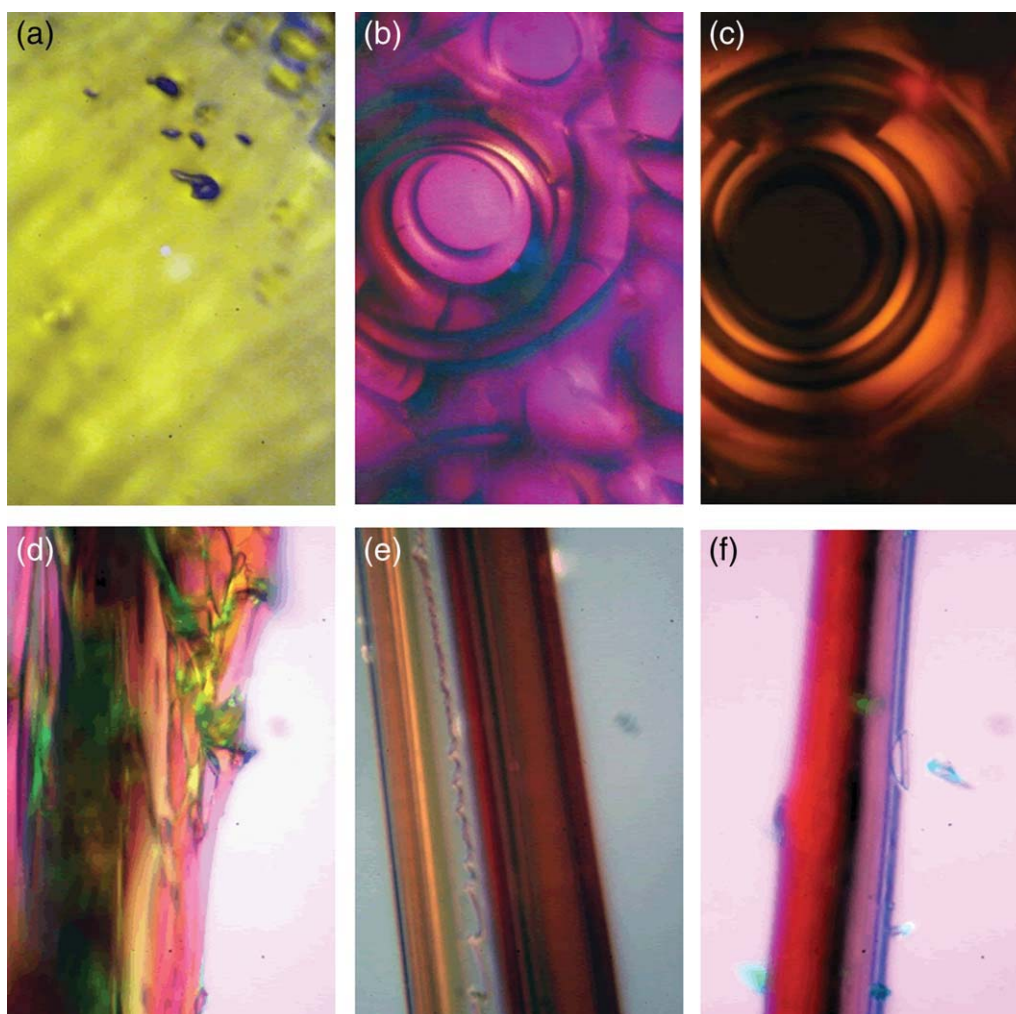


**FIGURE 3** Photomicrographs of (a) polymer **II-2**, (b) polymer **I-3**, and (c) polymer **II-3** exhibiting their glassy phases; and those of (d) polymer **II-2**, (e) polymer **I-3**, and (f) polymer **II-3** exhibiting hand-drawn fiber morphologies.

may be an indication of thermotropic LC phase as observed in previously reported poly(pyridinium salt)s.<sup>11h</sup> From the melt of these poly(pyridinium salt)s, we were able to draw thin fibers with thickness ranging from about 50 to 300  $\mu\text{m}$ . Figure 3(d–f) shows photomicrographs of fibers from polymers **II-2**, **I-3**, and **II-3**, respectively. In Figure 3(d), the fiber from polymer **II-2** shows quite rough surface with some voids and furrows. On the other hand, fibers from polymers **I-3** and **II-3** [Fig. 3(e,f)] have smoother surfaces even though some imperfections were also evident. To further elucidate the morphologies of these fibers, we examined them with SEM [Fig. 4(a–d)]. The fiber prepared from polymer **II-1** [Fig. 4(a)] is flat with a distinctive texture on its surface, while inside it seemed quite uniform. In contrast, the fiber produced from polymer **I-2** [Fig. 4(b)] has a smooth surface, while inside it there are numerous hollow cavities. In Figure 4(c), fiber from polymer **II-2** also has some roughness to the surface. The internal structure of this fiber are revealing where the surface is thinned out. It appears to have some hollowness similarly to the fiber made from polymer **I-2**. As these two polymers have the same backbone, this interesting

morphology, exhibited by both them, is presumably due the molecular structure of their backbones. The fiber prepared from polymer **I-3** is flat in nature similar to that of the fiber from polymer **I-1** but it also has smooth surface [Fig. 4(d)] and seemed filled and uniform in the cross-section (not shown). Next, we examined these materials with TEM studies. The samples were prepared from dilute solutions (1–5 wt %) of these polymers in either methanol or acetonitrile. Each of the triflimide polymers (**II-1–II-2**) exhibited an aggregated structure of unidentifiable nature as observed in Figure S23. On the other hand, the tosylate polymers (**I-1–I-3**) had quite distinct, different morphology as displayed in Figure 4(e,f). Polymer **I-2** formed a small spheroid clusters [Fig. 4(e)], whereas polymer **I-3** formed an interesting interconnected networks of spheroid objects [Fig. 4(f)]. The formation of spheroid objects of these ionic polymers are presumably related to the aggregation phenomenon, which may also related to the formation of lyotropic phase of these polymers. The aggregation phenomena of ionic polymers, irrespective of the nature of polyions either rigid-rod or flexible, in water or in organic solvents are quite remarkable in

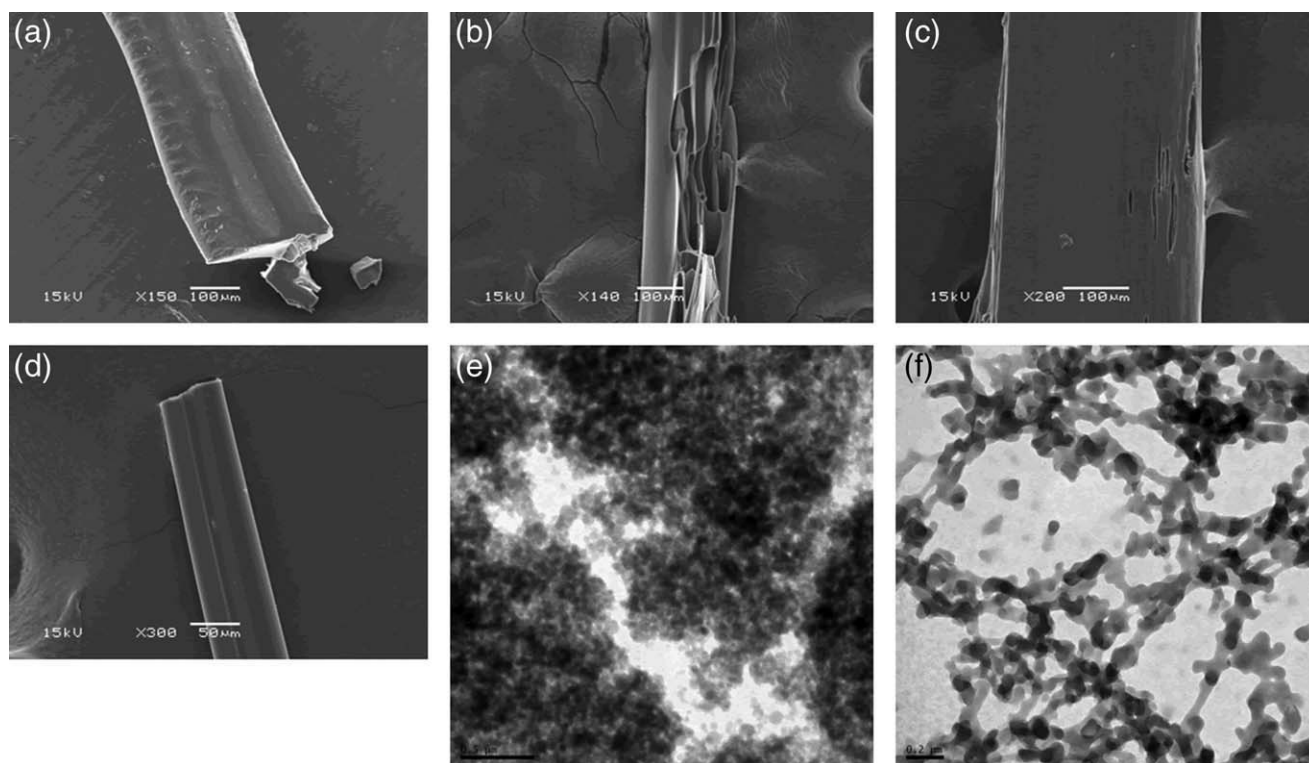


**FIGURE 4** SEM images of (a) polymer II-1, (b) polymer I-2, (c) polymer II-2, and (d) polymer I-3 exhibiting their fiber morphologies; and TEM images of (e) polymer I-2 (magnification 3,900 $\times$ ) from 5 wt % CH<sub>3</sub>OH solution and (f) polymer I-3 (magnification 5,000 $\times$ ) from 2 wt % CH<sub>3</sub>OH solution exhibiting aggregated particles.

general, because the macroions approach one another leading to the formation of aggregates instead of repulsion between like charges. The mechanism of this aggregation process remains unknown to date, but aggregation processes do occur in both flexible and rod-like polyelectrolytes as detected by various experimental techniques including optical microscopy, dynamic and static light scattering, X-ray scattering, scanning force microscopy and TEM, among others.<sup>17</sup> However, here we presented some interesting morphology of this class of poly(pyridinium salt)s in different conditions, which could shed light how these polymers will perform when they are used for the fabrication of functional devices.

## CONCLUSIONS

Several poly(pyridinium salt)s with tosylate and triflimide counterions, having pyridine diamine moieties, were prepared by ring-transmutation polymerization or metathesis reaction. Their chemical structures were verified by spectroscopic techniques including FTIR, NMR spectroscopy, and elemental analysis. Their intrinsic viscosities were as low as 0.05 dL/g and as high as 1.23 dL/g and their weight-average molecular weights ( $M_w$ ) were in a range of 11,000 to 110,000 as determined by GPC. All of these polymers had high thermal stabilities  $>340$  °C for the tosylate polymers and  $>427$  °C for the triflimide ones. As determined by DSC and XRD, these polymers are amorphous with high  $T_g$ s. They were highly soluble in common organic solvents, which is

essential for their fabrication into thin films by spin coating techniques or inkjet printing. Additionally, in several of these polymers, a fully grown lyotropic phase was developed in methanol, acetonitrile and DMSO and, therefore, much like Kevlar, these polymers could be processed into high-performance materials.<sup>13</sup>

They exhibited light-emitting properties in solvents of various polarities as well as in solid states. In solution they exhibited photoluminescence in the green region of visible light and their FWHM values were quite broad. Changing from solution to solid state, they generally exhibited hypsochromic shifts of about 20–30 nm, which suggested less ordered structures in film states compared to solution states. Exchange of the counterion from tosylate to triflimide did not affect the light emission in solutions but did affect this property in solid states of these polymers. They also showed reasonable quantum yields comparable to other  $\pi$ -conjugated LEPs.<sup>1</sup> They showed interesting morphologies in films and fibers as examined with POM, SEM, and TEM studies.

As they contain positively charged nitrogen ions that are associated with counterions in their backbones, they could also be used for light-emitting electrochemical cells.<sup>18</sup> Moreover, their thermal and optical properties could be fine tuned by exchange of the counterion to other counterions as required without the need of synthesizing new polymers. Finally, these ionic polymers could be used as polycations with appropriate polyanions to produce multilayered

nanoassemblies by either dipping or spin-assisted method to create functional materials.<sup>19</sup>

P.K.B. acknowledges the University of Nevada Las Vegas (UNLV) for New Investigation Award (NIA), Planning Initiative Award (PIA), and Applied Research Initiative (ARI) grants, and the donors of the Petroleum Research Fund, administered by the American Chemical Society, and an award (CCSA# CC5589) from Research Corporation for the support of this research. A.K.N. acknowledges the Graduate College (UNLV) for providing him a Nevada Stars Graduate Assistantship for the period of 2006–2008. The authors also sincerely acknowledge to Dr. Longzhou Ma for his expertise in the analyses of TEM studies.

## REFERENCES AND NOTES

- (a) Burroughes, J. H.; Bradley, D. D. C.; Brown, A. R.; Marks, R. N.; Mackay, K.; Friend, R. H.; Burns, P. L.; Holmes, A. B. *Nature* 1990, 347, 539–541; (b) Kraft, A.; Grimsdale, A. C.; Holmes, A. B. *Angew Chem Int Ed* 1998, 37, 402–428; (c) Friend, R. H.; Gymer, R. W.; Holmes, A. B.; Burroughes, J. H.; Marks, R. N.; Taliani, C.; Bradley, D. D. C.; Santos, D. A. D.; Bredas, J. L.; Logdlund, M.; Salaneck, W. R. *Nature* 1999, 397, 121–128; (d) Mitschke, U.; Bauerle, P. *J Mater Chem* 2000, 10, 1471–1507; (e) Akcelrud, L. *Prog Polym Sci* 2003, 28, 875–962; (f) McGehee, M. D.; Heeger, A. J. *Adv Mater* 2000, 12, 1655–1668; (g) Yeh, K.-M.; Lee, C.-C.; Chen, Y. *J Polym Sci Part A: Polym Chem* 2008, 46, 5180–5193; (h) Koga, Y.; Matsubara, K. *J Polym Sci Part A: Polym Chem* 2009, 47, 4358–4365; (i) Mishra, S. P.; Palai, A.; Srivastava, R.; Kamalasanan, M. N.; Patri, M. *J Polym Sci Part A: Polym Chem* 2009, 47, 6514–6525.
- (a) Wang, Y. Z.; Epstein, A. J. *Acc Chem Res* 1999, 32, 217–224; (b) Hong, H.; Sfez, R.; Vaganova, E.; Yitzchaik, S.; Davidov, D. *Thin Solid Films* 2000, 366, 260–264; (c) Wang, C.; Kilitziraki, M.; MacBride, J. A. H.; Bryce, M. R.; Horsburgh, L. E.; Sheridan, A. K.; Monkman, A. P.; Samuel, I. D. W. *Adv Mater* 2000, 12, 217–222.
- (a) Hoshino, S.; Ebata, K.; Furukawa, K. *J Appl Phys* 2000, 87, 1968–1973; (b) Janietz, S.; Anlauf, S.; Wedel, A. *Macromol Chem Phys* 2002, 203, 433–438; (c) Adachi, C.; Baldo, M. A.; Forrest, S. R.; Thompson, M. E. *App Phys Lett* 2000, 77, 904–906; (d) Wang, S.; Wu, P.; Han, Z. *Macromolecules* 2003, 36, 4567–4576; (e) Herguth, P.; Jiang, X.; Liu, M. S.; Jen, A. K. Y. *Macromolecules* 2002, 35, 6094–6100; (f) Monkman, A. P.; Palsson, L.-O.; Higgins, R. W. T.; Wang, C.; Bryce, M. R.; Batsanov, A. S.; Howard, J. A. K. *J Am Chem Soc* 2002, 124, 6049–6055; (g) Hancock, J. M.; Gifford, A. P.; Tonzola, C. J.; Jenekhe, S. A. *J Phys Chem C* 2007, 111, 6875–6882; (h) Zhang, X.; Jenekhe, S. A. *Macromolecules* 2000, 33, 2069–2082; (i) Stille, J. K. *Macromolecules* 1981, 14, 870–880.
- Kulkarni, A. P.; Tonzola, C. J.; Babel, A.; Jenekhe, S. A. *Chem Mater* 2004, 16, 4556–4573.
- Tamami, B.; Yeganeh, H.; Kohmareh, G. A. *Eur Polym J* 2004, 40, 1651–1657.
- Li, L.; Kikuchi, R.; Kakimoto, M.-A.; Jikei, M.; Takahashi, A. *High Perform Polym* 2005, 17, 135–147.
- (a) Behniafar, H.; Banihashemi, A. *Eur Polym J* 2004, 40, 1409–1415; (b) Behniafar, H.; Banihashemi, A. *Polym Int* 2004, 53, 2020–2025; (c) Behniafar, H.; Mirzai, A. A. K.; Saeed, A. B. *Polym Int* 2007, 56, 74–81.
- (a) Liaw, D.-J.; Wang, K.-L.; Chang, F.-C. *Macromolecules* 2007, 40, 3568–3574; (b) Liaw, D.-J.; Wang, K.-L.; Chang, F.-C.; Lee, K.-R.; Lai, J.-Y. *J Polym Sci Part A: Polym Chem* 2007, 45, 2367–2374.
- Katritzky, A. R.; Brownlee, R. T. C.; Musumarra, G. *Tetrahedron* 1980, 36, 1643–1647.
- (a) Harris, F. W.; Chuang, K. C.; Huang, S. A. X.; Janimak, J. J.; Cheng, S. Z. D. *Polymer* 1994, 35, 4940–4948; (b) Huang, S. A. X.; Chuang, K. C.; Cheng, S. Z. D.; Harris, F. W. *Polymer* 2000, 41, 5001–5009.
- (a) Bhowmik, P. K.; Burchett, R. A.; Han, H.; Cebe, J. J. *Macromolecules* 2001, 34, 7579–7581; (b) Bhowmik, P. K.; Burchett, R. A.; Han, H.; Cebe, J. J. *J Polym Sci, Part A: Polym Chem* 2001, 39, 2710–2715; (c) Bhowmik, P. K.; Han, H.; Cebe, J. J.; Nedeltchev, I. K.; Kang, S.-W.; Kumar, S. *Macromolecules* 2004, 37, 2688–2694; (d) Bhowmik, P. K.; Han, H.; Nedeltchev, A. K. *Polymer* 2006, 47, 8281–8288; (e) Bhowmik, P. K.; Han, H.; Nedeltchev, A. K. *J Polym Sci Part A: Polym Chem* 2006, 44, 1028–1041; (f) Bhowmik, P. K.; Kamatam, S.; Han, H.; Nedeltchev, A. K. *Polymer* 2008, 49, 1748–1760; (g) Bhowmik, P. K.; Han, H.; Nedeltchev, A. K.; Mandal, H. D.; Jimenez-Hernandez, J. A.; McGannon, P. M. *Polymer* 2009, 50, 3128–3135; (h) Bhowmik, P. K.; Han, H.; Nedeltchev, A. K.; Mandal, H. D.; Jimenez-Hernandez, J. A.; McGannon, P. M. *J Appl Polym Sci* 2010, 116, 1197–1206; (i) Nedeltchev, A. K.; Han, H.; Bhowmik, P. K. *Polym Chem* 2010, 1, 908–915.
- Fery-Forgues, S.; Lavabre, D. *J Chem Ed* 1999, 76, 1260–1264.
- (a) Tanner, D.; Fitzgerald, J. A.; Phillips, B. R. *Angew Chem Int Ed* 1989, 28, 649–654; (b) Lin, J.; Sherrington, D. *Adv Polym Sci* 1994, 111, 177–219; (c) Keating, M. Y. *Thermochim Acta* 1998, 319, 201–212.
- (a) Shirota, Y. *J Mater Chem* 2000, 10, 1–25; (b) Shirota, Y. *J Mater Chem* 2005, 15, 75–93; (c) Shirota, Y.; Kageyama, H. *Chem Rev* 2007, 107, 953–1010.
- Liou, G.-S.; Yang, Y.-L.; Su, Y. O. *J Polym Sci Part A: Polym Chem* 2006, 44, 2587–2603.
- Greaves, T. L.; Drummond, C. J. *Chem Rev* 2008, 108, 206–237.
- (a) Tanahatue, J. J.; Kuil, M. E. *J Phys Chem B* 1997, 101, 5905–5908; (b) Kroeger, A.; Deimede, V.; Belak, J.; Lieberwirth, I.; Fytas, G.; Wegner, G. *Macromolecules* 2007, 40, 105–115; (c) Bhowmik, P. K.; Cheney, M. A.; Jose, R.; Han, H.; Banerjee, A.; Ma, L.; Hansen, L. D. *Polymer* 2009, 50, 2393–2401.
- (a) Bernards, D. A.; Flores-Torres, S.; Abruña, H. D.; Malliaras, G. G. *Science* 2006, 313, 1416–1419; (b) Mauthner, G.; Landfester, K.; Köck, A.; Brückl, H.; Kast, M.; Stepper, C.; List, E. J. W. *Org Electron* 2008, 9, 164–170.
- (a) Decher, G. *Science* 1997, 277, 1232–1237; (b) Lefaux, C. J.; Zimmerlin, J. A.; Dobrynin, A. V.; Mather, P. T. *J Polym Sci Part B: Polym Phys* 2004, 42, 3654–3666.